

Effects of single-particle potentials on the level density parameter

B. Canbula, R. Bulur, D. Canbula and H. Babacan

Department of Physics, Faculty of Arts and Sciences, Celal Bayar University, 45140, Muradiye, Manisa, Turkey

Received: date / Revised version: date

Abstract. The new definition of the energy dependence for the level density parameter including collective effects depends strongly on the semi-classical approach. For this method, defining an accurate single-particle potential is of great importance. The effect of the single-particle potential terms, which are central, spin-orbit, harmonic oscillator, Woods-Saxon and Coulomb potential, both for spherical and deformed cases, on the level density parameter was investigated by examining the local success of the global parameterizations of eight different combinations of these terms. Among these combinations, the sum of the central, spin-orbit, harmonic oscillator and Coulomb potentials, gives the most accurate predictions compared with experimental data. The local selections of the global parameterizations show that the single-particle models, which are based on Woods-Saxon potential as the main term, are more suitable candidates than the models based on harmonic oscillator potential to extrapolate away far from stability. Also it can be concluded that the contribution of the Coulomb interaction, both around the closed and open shells is not neglectable.

PACS. 21.10.Ma Level density – 21.10.Re Collective levels

1 Introduction

The number of the excited states in an infinitesimal amount of energy around a certain excitation energy is called as the nuclear level density (NLD). The NLD is of vital importance for the theoretical studies of nuclear structure and reactions. The excited levels of the nucleus are very scarce at low excitation energy and can be countable easily, but with the increasing excitation energy, it is not possible to count the levels since the spacing between consecutive levels becomes so narrow. Therefore, a function is needed to describe the distribution of the excited levels, which is very important for the Hauser-Feshbach calculations of the compound-nucleus cross sections.

To develop a theoretical framework for understanding the unusual properties of the light exotic beams has been of major interest during the last few decades [1]. Even though very sophisticated nuclear reaction models [2,3,4,5,6,7,8,9,10,11], which give accurate predictions in many cases, have been developed, in the solution of this complex problem, structural properties, such as the distribution of their excited levels, arising from both pure single-particle and collective excitations, should be also considered. Thus, correct description of NLD containing these effects is also required to explain the reaction data.

A Laplace-like formula for the level density parameter including collective effects has been proposed in our recent paper [12]. The new definition of the energy dependence for the level density parameter significantly improved the agreement between predicted and observed excited energy

levels. Furthermore, the asymptotic level density parameter, \tilde{a} , is redescribed in a both more physical and more realistic way. This redescription takes into account corrections for both the shell and pairing effects in addition to the value obtained from the semi-classical approximation analytically or numerically. Using the semi-classical approximation [13] requires a well-defined single-particle potential because it directly determines \tilde{a} , which is the limit value of the level density parameter for the energies above the neutron separation energy. Therefore, the single-particle potential almost remains the only component to improve the success of the reaction calculations that uses the level density as an ingredient. In other words, the single-particle potential parameterization is still of great importance for the level density.

In our previous work [12], we have performed the global and the local calculations to obtain \tilde{a} . In global calculation, we used the single-particle potential consists of harmonic oscillator, Coulomb and central potential terms with global potential parameters. In contrast, the local calculation considers the asymptotic level density parameter as a free parameter to be adjusted to the experimental data on the mean resonance spacing and discrete level scheme for each nuclei separately. Although, as expected, locally adjusted values of the asymptotic level density parameter provide much better agreement with the experimental data as compared with the global parameterization, disregarding of the global potential parameters is not permissible, especially, for the nuclei near the driplines. Since there is not enough experimental information on the excited energy levels of these nuclei, this situation makes

Correspondence to: bora.canbula@cbu.edu.tr

impossible to adjust the asymptotic level density parameter locally, and therefore, to rely on a global parameterization becomes an obligation rather than a choice.

There are nearly 2000 nuclei, which have at least two experimentally-known excited energy levels [14]. It seems that the global potential which has the highest predictive power is harmonic oscillator with Coulomb and central terms for all these nuclei over the whole mass range [12]. However, various combinations of potential terms can be more suitable in certain mass regions. Moreover, there can be possible correlations between the potential choice and some other properties of nuclei, not only their mass number. In this manner, it is worth to investigate that the behavior of the goodness-of-fit estimators, which results from the global parameterizations of different single-particle potentials, with respect to some fundamental properties as well as the mass number of nuclei.

The aim of this paper is to investigate the role of the single-particle potential in the predictive power of the semi-classical level density model for eight different combinations of the potential terms by comparing the global parameterizations to each other and also by analyzing the local success of them. For this purpose, four different combinations are constructed on the basis of two main potentials, which are harmonic oscillator and Woods-Saxon, with and without Coulomb interaction combined with the central and spin-orbit term for all combinations. In addition to these potentials, we constructed four more combination to investigate the effect of deformation with anisotropic harmonic oscillator and deformed Woods-Saxon potentials as main potential terms.

The present paper is organized as follows: In Section 2, we briefly discuss the method used to obtain the asymptotic level density parameter \tilde{a} . Section 3 contains the definition of the goodness-of-fit estimators for phenomenological level density models. Then, in Section 4, we present the single-particle potentials, which we used in this work, and discuss our results for 1136 nuclei in Section 5. Finally, a summary of our model and some concluding remarks of this paper are given in Section 6.

2 Theory

Many studies of the nuclear level density have been based on the Fermi gas model [15] in which interactions between nucleons are ignored. Therefore, nucleons are assumed to occupy equispaced single-particle states arising from an average nuclear potential. According to this model, one can describe the level density at an excitation energy for a certain total angular momentum J and parity Π

$$\rho(U, J, \Pi) = \frac{1}{2} \frac{2J+1}{2\sqrt{2\pi}\sigma^3} \exp\left[-\frac{(J+\frac{1}{2})^2}{2\sigma^2}\right] \times \frac{\sqrt{\pi} \exp\left[2\sqrt{aU}\right]}{12 a^{1/4} U^{5/4}} \quad (1)$$

where the factor $\frac{1}{2}$ corresponds equiparity. The remaining ingredients a , U and σ^2 represent the level density param-

eter, the effective excitation energy and the spin cut-off parameter, respectively. For the Fermi gas model, the total level density is described by summing Eq. (1) over all spins

$$\rho^{\text{tot}}(E_x) = \frac{1}{\sqrt{2\pi}\sigma} \frac{\sqrt{\pi} \exp[2\sqrt{aU}]}{12 a^{1/4} U^{5/4}}. \quad (2)$$

The collective effects arising from the collective motion of many nucleons were not taken into account in the Fermi gas model. However, these effects play an important role in populating of the excited states. In the later studies [16, 17], collective effects have been considered as vibrational and rotational effects separately and included in the model as additional enhancement factors to total level density. In our recent work [12], we have introduced a Laplace-like formula for the energy dependence of the level density parameter which spread the collective effects through the whole level density calculation. The level density parameter a including collective effects is given by

$$a(U) = \tilde{a} \left(1 + A_c \frac{S_n \exp(-|U - E_0|/\sigma r_c^3)}{\sigma r_c^3} \right). \quad (3)$$

where S_n is the neutron separation energy. A_c is the collective amplitude and defined as the shape dependent shell (microscopic) correction energy at a critical temperature $T_c = \sqrt{S_n/\tilde{a}}$, which is the nuclear temperature at S_n ,

$$\begin{aligned} A_c &= S(N, Z, T_c, \text{Shape}) \\ &= [M_{\text{exp}} - M_{\text{LDM}}] \frac{\tau_c}{\sinh \tau_c} \\ &= [M_{\text{exp}} - (M_0 + E\theta^2)] \frac{\tau_c}{\sinh \tau_c}, \end{aligned} \quad (4)$$

where $\tau_c = 2\pi^2 T_c / \hbar\omega$. M_{LDM} is the calculated mass of the deformed nucleus from the shape dependent liquid drop model, where M_0 is the mass of the corresponding spherical nucleus. Thus, M_{LDM} can be calculated from the formula

$$M_{\text{LDM}} = M_N N + M_H Z + E_V + E_S + E_C \pm \frac{11}{\sqrt{A}} + E\theta^2 \quad (5)$$

of finite-range liquid-drop model [18]. The last term is due to small deformations and related to both fissility and deformation parameters as $E = (2/5)c_2 A^{2/3}(1-x)\alpha_0^2$ where $\alpha_0^2 = 5(a/r_0)^2 A^{-2/3}$, $\theta = \alpha/\alpha_0$, $\alpha^2 = (5/4\pi)\beta^2$, and $x = E_C/2E_S$. The values of the constants of the liquid drop model are taken as in Ref. [19]. As mentioned above, σ_c^2 is the spin cut-off parameter and is given as

$$\sigma_c^2 = \frac{T_c}{\hbar^2} 0.4MR^2 \left[1 + \sqrt{\frac{5\pi}{16}}\beta_2 + \frac{45\beta_2^2}{28\pi} + \frac{15\beta_2\beta_4}{7\sqrt{5\pi}} \right] \quad (6)$$

for deformed nuclei [16]. Where c indicates to its value at T_c , and $\sigma_c^3 = \sigma_c^3/\tilde{a}$ is the scale parameter for Laplace distribution, for further details see ref. [12]. E_0 is the energy of the first phonon level which corresponds to the first excited state caused by vibrational effects [20,21]. This energy level is also known as the first 2^+ excitation state

for even-even nuclei [21] and its energy can be given with a simple formula $0.2\hbar\omega$ fitted to experimental 2^+ states [22, 23]. Finally, \tilde{a} is the asymptotic level density parameter, which is crucial in the level density calculations and it is defined in different forms by many authors. The simplest expression of this parameter is given by [17, 24]

$$\tilde{a} = \frac{A}{k} \quad (7)$$

or can be taken as the liquid drop like formula [25]

$$\tilde{a} = a_{\text{vol}} \left[1 + k_{\text{vol}} \left(\frac{N-Z}{A} \right)^2 \right] A + a_{\text{sur}} \left[1 + k_{\text{sur}} \left(\frac{N-Z}{A} \right)^2 \right] A^{2/3} + a_{\text{Coul}} Z^2 A^{-1/3}. \quad (8)$$

Another expression for this parameter, fitting to resonance spacings and/or discrete levels, can be written as [26]

$$\tilde{a} = \alpha A + \beta A^{2/3}, \quad (9)$$

where α and β are adjustable parameters.

Unlike the above expressions, we used a modified expression of the well-known semi-classical formula [27, 28] for the asymptotic level density parameter in terms of the single-particle level density at Fermi energy of nucleus including the shell and pairing corrections [12]

$$\tilde{a} = \frac{\pi^2}{6} [g_p(E_F^p + S(N, Z) - \Delta) + g_n(E_F^n + S(N, Z) - \Delta)]. \quad (10)$$

$S(N, Z)$ denotes the shell correction energy from the liquid drop model [18]. The pairing correction energy is given by $\Delta = n \frac{12}{\sqrt{A}}$ with n is -1 for odd-odd, 1 for even-even, 0 for odd nuclei. Therefore, including the energy shift Δ to the Fermi energy substitutes the usage of the expression $U = E_x - \Delta$ and allows to use effective excitation energy U instead of pure excitation energy E_x directly. g_p and g_n are proton and neutron single particle level density, respectively, and can be calculated from the semi-classical formula with spin degeneracy [28, 29]

$$g(\varepsilon) = \frac{2}{\pi} \left(\frac{2m}{\hbar^2} \right)^{3/2} \int r^2 \sqrt{\varepsilon - V(r)} dr. \quad (11)$$

m is the mass of a nucleon and $V(r)$ is an effective potential. The proton and neutron Fermi energy values E_F^α can be obtained by inverting the integral, which gives the nucleon number in terms of single-particle level density

$$\mathcal{N}_\alpha = \int_{-\infty}^{E_F^\alpha} g_\alpha(E) dE, \quad \mathcal{N}_\alpha = \{N, Z\}. \quad (12)$$

Therefore, the crucial role of the single-particle potential in the asymptotic level density parameter motivated us to investigate the effects of the single-particle potential description to predictive power of the semi-classical level density model. For this purpose, we consider eight different combinations of various single-particle potential terms and analyze the results in the view of agreement between their predictions and observations.

3 Goodness-of-fit Estimators

Phenomenological level density models have been needed to agree with two observable, which are average resonance spacings and discrete level schemes. One can test the reliability of the level density models with the aid of these observable. In this study, we have calculated the rms deviation factor of the mean resonance spacings for 289 nuclei, which exist naturally on Earth, and their experimental average resonance spacing data are available. However, the average goodness-of-fit estimator of discrete levels for 1136 nuclei, which have sufficient information on the discrete energy level scheme. The goodness-of-fit estimator χ^2 for average resonance spacings has been minimized to follow as

$$\chi_{D,i}^2 = \left(\frac{D_{0,i}^{\text{theo}} - D_{0,i}^{\text{exp}}}{D_{0,i}^{\text{err}}} \right)^2, \quad (13)$$

where the index i indicates the nucleus. $D_{0,i}^{\text{exp}}$ and $D_{0,i}^{\text{err}}$ are respectively experimental data and the uncertainty of the average resonance spacing which its theoretical predictions are obtained from the equation below

$$\frac{1}{D_0^{\text{theo}}} = \sum_{J=|I-\frac{1}{2}|}^{J=I+\frac{1}{2}} \rho(S_n, J, \Pi). \quad (14)$$

Unlike the average resonance spacings, goodness-of-fit estimator for discrete levels has no experimental error in the cumulative level scheme and is given by

$$\chi_{\text{lev},i}^2 = \sum_{k=N_L^i}^{N_U^i} \frac{[N_{\text{cum}}^i(E_k) - k]^2}{k}. \quad (15)$$

Here, k represents the sum over the discrete levels and the cumulative number of levels N_{cum} up to an excitation energy E is calculated from

$$N_{\text{cum}}(E) = N_L + \int_{E_L}^E \rho^{\text{tot}}(E_x) dE_x. \quad (16)$$

These estimators allow us to test the agreement between our predictions and experimental data besides making comparisons with the results of the other level density models. The rms deviation factor of mean resonance spacings, which is defined as for all N nuclides reads

$$f_{\text{rms}} = \exp \left[\frac{1}{N} \sum_{i=1}^N \left(\ln \frac{D_{0,i}^{\text{theo}}}{D_{0,i}^{\text{exp}}} \right)^2 \right]^{1/2} \quad (17)$$

and the average goodness-of-fit estimator for discrete levels is

$$f_{\text{lev}} = \frac{1}{N} \sum_{i=1}^N \sum_{k=N_L^i}^{N_U^i} \frac{[N_{\text{cum}}^i(E_k) - k]^2}{k}. \quad (18)$$

4 Single-Particle Potentials

In our recent work [12], we have calculated the nuclear level density parameter by using the semi-classical approximation with the single-particle potential consists of harmonic oscillator and central potential terms and also Coulomb potential for protons. That study [12] leads us to investigate the single-particle potential's role of choosing the best agreement for each nuclei in level density calculations. In this study, we used various single-particle potential terms, which are central, harmonic oscillator, Woods-Saxon, Coulomb, and spin-orbit potentials. We have considered eight different combinations constructed from these single-particle potential terms:

$$V(r) = V_{\text{central}}(r) + V_{\text{main}}(r) + V_{\text{Coulomb}}(r) + V_{\text{SO}}. \quad (19)$$

The central potential is taken into account for all potential combinations and is given by the equation below

$$V_{\text{central}}(r) = \hbar^2 l(l+1)/2mr^2 \quad (20)$$

where l is the angular momentum. Also spin-orbit potential, which is very important for the structure of the single-particle states near the Fermi surface, is considered in all combinations and usually reads [22]

$$V_{\text{SO}}(r) = \lambda \frac{1}{r} \frac{dV}{dr} (\mathbf{l} \cdot \mathbf{s}). \quad (21)$$

where $\lambda \approx -0.5 \text{ fm}^2$. However, using harmonic oscillator potential leads a constant spin-orbit term. Therefore, we prefer here a radius-independent form given as [30],

$$V_{\text{SO}} = C \hbar^2 (\mathbf{l} \cdot \mathbf{s}) \quad (22)$$

for all combinations in order to ensure consistency. The constant C for spin-orbit potential is typically in the range of -0.3 to $-0.6 \text{ MeV}/\hbar^2$. We take $C = -0.3 \text{ MeV}/\hbar^2$ in our calculations, arbitrarily.

As the main potential, we used harmonic oscillator (HO) or Woods-Saxon (WS) potential both in their spherical and deformed forms. The HO potential, which has a very convenient form for analytical calculations, is described as follows

$$V_{\text{HO}}(r) = \frac{1}{2} m \omega^2 r^2 - V_0 \quad (23)$$

where ω is the oscillator frequency, and it has been generally parameterized as $41/A^{1/3}$. The depth of the potential well, V_0 , is taken as 50 MeV [27]. These parameters are chosen to represent only the common properties of the nuclei because the other effects like shell and pairing corrections will be applied to Fermi energy explicitly as in Eq. (10). In order to deal with the deformation of the nucleus, anisotropic harmonic oscillator

$$V_{\text{HO}}^{\text{def}}(x, y, z) = \frac{1}{2} m (\omega_x^2 x^2 + \omega_y^2 y^2 + \omega_z^2 z^2) - V_0 \quad (24)$$

is employed. When z-axis is chosen as symmetry axis, one can define the oscillator frequencies for axially symmetric shapes in terms of the deformation parameter δ

$$\begin{aligned} \omega_{\perp}^2 &= \omega_x^2 = \omega_y^2 = \omega_0^2(\delta) \left(1 + \frac{2}{3}\delta\right) \\ \omega_z^2 &= \omega_0^2(\delta) \left(1 - \frac{4}{3}\delta\right). \end{aligned} \quad (25)$$

$\omega_0(\delta)$ is obtained by using the volume conservation and reads

$$\omega_0(\delta) = \omega_0 \left[1 - \frac{4}{3}\delta^2 - \frac{16}{27}\delta^3 \right]^{-1/6} \quad (26)$$

where δ is related to β in Eq. (5) as follows [22]:

$$\beta \approx \frac{1}{3} \sqrt{\frac{16\pi}{5}} \delta \approx 1.057\delta. \quad (27)$$

The other option for the main potential is the WS potential, which is a more realistic description compared to HO meanwhile to use WS in calculations causes some difficulties due to the inability to obtain analytical solutions. The WS potential is written as

$$V_{\text{WS}}(r) = -\frac{V_0}{1 + \exp\left(\frac{r-R}{a}\right)}. \quad (28)$$

V_0 , R and a are depth, radius and diffuseness parameters of the potential well, respectively. In this study, potential well depth is taken as 50 MeV to be consistent with the HO potential, and radius is defined as $R = r_0 A^{1/3}$ where r_0 equals 1.25 fm . Also, diffuseness parameter of the potential well is used as 0.5 fm in calculations. For WS potential, the deformation can be included in the parameter R as

$$R(\theta, \phi) = (r_0 A^{1/3}) \left[1 + \sum_{\lambda} \sum_{\mu} a_{\lambda\mu} Y_{\lambda\mu}(\theta, \phi) \right], \quad (29)$$

related to deformation parameter as $\beta^2 = \sum_{\lambda} \sum_{\mu} |a_{\lambda\mu}|^2$ [18]. Therefore, WS potential for the deformed nuclei is expressed as follows:

$$V_{\text{WS}}^{\text{def}}(r, \theta, \phi) = -\frac{V_0}{1 + \exp\left(\frac{r-R(\theta, \phi)}{a}\right)}. \quad (30)$$

Furthermore, the potential combination consisting of the central and spin-orbit potential terms and the selected main potential is complemented with Coulomb potential for protons to investigate Coulomb interaction on the level density parameter. Under the assumption that nucleus is a uniformly charged sphere, the Coulomb potential is given by

$$V_C(r) = \begin{cases} \frac{Ze^2}{2R_C} \left(3 - \frac{r^2}{R_C^2} \right) & r \leq R_C \\ \frac{Ze^2}{r} & r \geq R_C \end{cases} \quad (31)$$

where R_C is charge radius and is taken as $R_C = 1.169 A^{0.291}$ from a recent fit [31] to the latest nuclear charge radii data [32].

Table 1. (Color online) Goodness-of-fit estimator values for various potential combinations and comparison with previous results.

Model	Potential Terms	f_{rms}	f_{lev}	Reference
Model 0	● Local Selections	1.30	1.00	This work
Model 1	● Central + SO + HO	1.63	1.91	This work
Model 2	● Central + SO + HO + Coulomb	1.51	1.32	This work
Model 3	● Central + SO + WS	2.06	1.65	This work
Model 4	● Central + SO + WS + Coulomb	2.11	1.70	This work
Model 5	● Central + SO + Deformed HO	1.66	1.71	This work
Model 6	● Central + SO + Deformed HO + Coulomb	1.55	1.31	This work
Model 7	● Central + SO + Deformed WS	1.74	1.62	This work
Model 8	● Central + SO + Deformed WS + Coulomb	2.24	1.80	This work
	Central + HO + Coulomb	1.53	1.32	[12]
	HO	1.12	43.9	[13]
	HO + Coulomb	1.16	42.6	[13]

However, one would note that the first single-particle level has never been in the bottom of the potential well, and this situation should be considered when calculating the Fermi energy level. Therefore, the contribution from the interval between the bottom of the potential well and the first single-particle level with the lowest energy should be zero in the integral (12). The value of the first single-particle level is well known for the HO potential but to make a similar prediction for WS potential might be difficult. So, considering that the total depth of the well is approximately equal to the sum of the Fermi energy and binding energy [27], to determine a value for this interval is a reasonable correction which has applied as first 8 MeV for the WS potential.

5 Results and Discussion

Using the single-particle potential terms given in Section 4, we define eight different combinations, which are labelled as Model 1 to 8. Table 1 includes these model definitions with their f_{rms} and f_{lev} values, which are calculated for 1136 nuclei using Eqs. (17) and (18), respectively, and also shows the results of our preceding studies [12,13]. The unique difference between Model 2 and the single-particle potential used in Ref. [12] is the spin-orbit term, which improves the predictive power of the model. When this model compared our another study [13], two remarkable differences exist in model definitions. In this study, we replace the simple description ($R_C = 1.2 A^{1/3}$) of the charge radius with an expression obtained in a recent fit [31], and also use Laplace-like formula instead of well-known Ignatyuk's formula [33] for level density parameter. These modifications lead to a significant improvement in the agreement between the predicted cumulative number of levels and the observed number of excited levels.

As the model predictions are compared with each other, Model 2 gives the most accurate model for the entire mass range. Moreover, it can be seen that HO based models are more predictive than WS based models, but among them only Model 7, which takes into account the deformation of the nucleus, is comparable with HO based models. It is an unexpected result because WS potential is more realistic

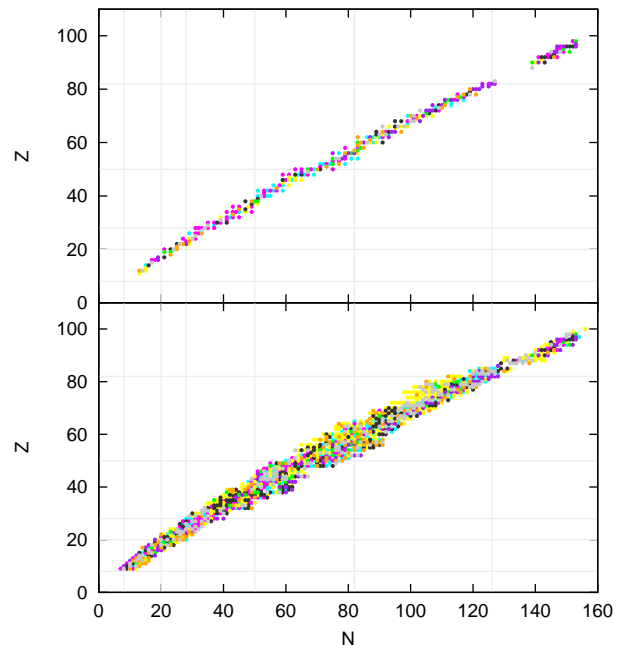


Fig. 1. (Color online) The local selections of the single-particle combinations. The upper panel includes 289 stable isotopes while the lower panel includes 1136 isotopes. Cyan, yellow, magenta, black, green, purple, orange and gray colored dots donate Models 1 to 8, respectively. The magic numbers are shown with grid lines.

than HO potential. This fact led us to a further analysis. On the other hand the comparison between these eight models only gives a general idea about their success to describe the common properties of the most of the nuclei. But in the case of the extrapolation to certain mass regions, especially near the driplines, this point of view becomes deficient. Therefore, testing the predictions of the global potential parameterizations locally for each nuclei might be the only useful method to conclude that which potential model is suitable to extrapolate outside the certain mass regions.

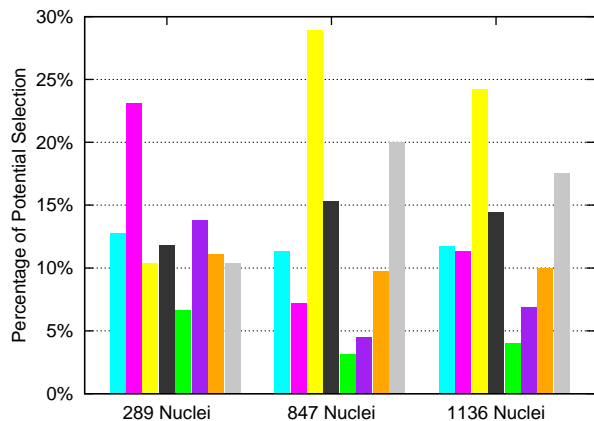
Table 2. Details of the selections of Model 0. The first line represents 289 stable isotopes. The third line represents 1136 isotopes while the selections of the remaining 847 isotopes are given in the second line.

NoI	NoI	%	NoI	%	NoI	%	NoI	%	NoI	%	NoI	%	NoI	%		
	Model 1		Model 2		Model 3		Model 4		Model 5		Model 6		Model 7	Model 8		
289	37	12.8	67	23.1	30	10.4	34	11.8	19	6.6	40	13.8	32	11.1	30	10.4
847	96	11.3	61	7.2	245	28.9	130	15.3	26	3.1	38	4.5	82	9.7	169	20.0
1136	133	11.7	128	11.3	275	24.2	164	14.4	45	4.0	78	6.9	114	10.0	199	17.5
	Model 1+2		Model 3+4		Model 5+6		Model 7+8		Model 1+5		Model 2+6		Model 3+7	Model 4+8		
289	104	35.9	64	22.2	59	20.4	62	21.5	56	19.3	107	37.0	62	21.5	64	22.2
847	157	18.5	375	44.2	64	7.6	251	29.7	122	14.4	99	11.7	327	38.6	299	35.3
1136	261	23.0	439	38.6	123	10.9	313	27.5	178	15.7	206	18.2	389	34.2	363	31.9
	Model 1+2+5+6				Model 3+4+7+8				Model 1+2+3+4				Model 5+6+7+8			
289					163	56.4					126	43.6				
847					221	26.1					626	73.9				
1136					384	33.9					700	61.6				

NoI stands for number of isotopes.

Considering these two aspects, we define Model 0, which consists of the local selections among the global parameterizations of Models 1-8. In Model 0, the selections have been made to give the lowest χ_i^2 contribution to global χ^2 values for the considered nucleus. Local model selections chosen with this criterion are illustrated in the upper and lower panels of Figure 1 for 289 and 1136 nuclei, respectively. The local model selections of 289 stable isotopes of the total of 1136 isotopes are shown explicitly in the upper panel because of the interpretations about the stable isotopes might be completely different from the rest. Consistent with the above discussion of Table 1, for stable isotopes, most of the selections are in HO based models. Models 2 and 6 are the almost only options in the heavy mass, $Z > 70$, region. Therefore, it can be said that the effect of the Coulomb interaction becomes indispensable with the increasing proton number, specially in this region. Also in $Z < 40$ region, Model 2 selections are quite intense compared to other models. However, in the case of 1136 isotopes, a significant increase has been noted in the number of selections of WS based models. These selections are notably more abundant in the region covering the exterior side of the island shown in the lower panel of Figure 1.

On the other hand, quantifying the total numbers of selections of models might be useful to conclude that which model is better to extrapolate to far from stability. Table 2 shows this quantification. Besides Models 1-8, the cumulative number of selections of models based on the same kind of potential terms are also shown in Table 2. The local selections of 289 stable isotopes, and the remaining 847 isotopes seem to be completely different from each other. This issue is also emphasized in Figure 2. For 289 stable isotopes WS based models have been selected only 43.6 percent of total selections. However, for remaining 847 isotopes, selection rate increases to 73.9 percent. In contrast to overwhelming superiority of Model 2, which is clearly seen from Table 1, WS based models, especially Model 3, seem to have had considerable success in describing the properties of the isotopes far from stability. Moreover, in the case of 1136 isotopes, the total numbers

**Fig. 2.** (Color online) The bar chart of the selections of Model 0. The color codes are the same as Figure 1 and Table 1.

of selections of WS based models are slightly greater than that of HO based models. When the selections are expanded from 289 isotopes to 1136, Model 2, which is the most selected model, falls back to fifth place. Therefore, it can be concluded that HO potential is very suitable for describing the most of the nuclei, but some certain isotopes or mass regions can be described better with WS potential. Nevertheless, WS potential is not suitable for a generalization to the entire mass region, at least with the potential parameters used in this work.

The asymptotic level density parameter values obtained by using Models 1-8 are illustrated in Figure 3. The first impression that emerges from Figure 3, for all models there exists the downwards peaks around the closed shells arising from the shell effects. However, there are also upwards peaks around the open shells only for Models 3 and 4 (WS based spherical models). In addition, the Coulomb term seems to increase the depth and the height of these peaks.

In Figure 4 the asymptotic level density parameter values of Model 0 are plotted. The color codes correspond to the single-particle potential models used for calculating the asymptotic level density parameter. Models based on

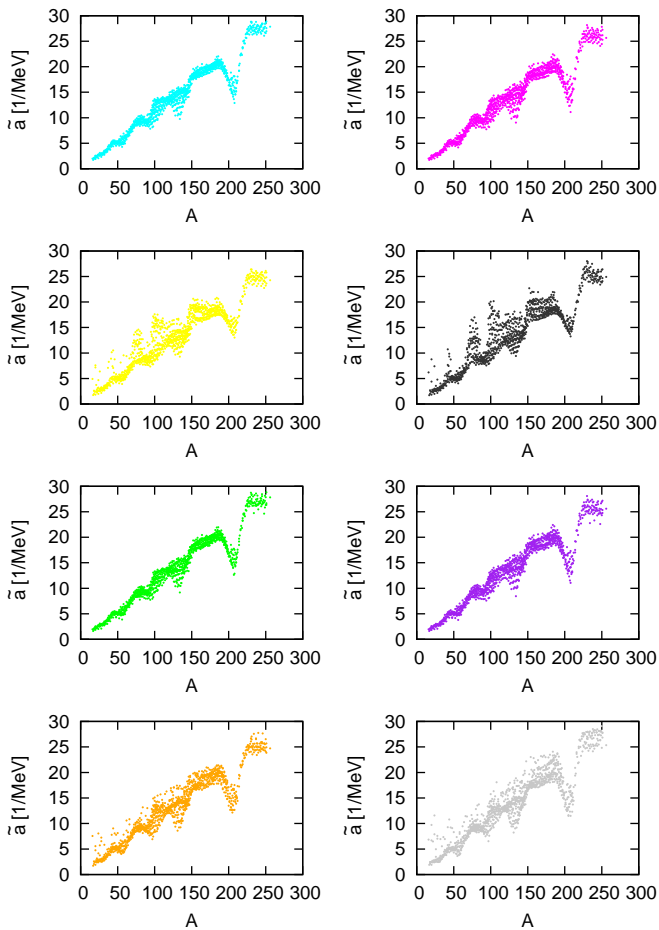


Fig. 3. (Color online) The asymptotic level density parameter values obtained by using eight different single particle potential combinations for 1136 isotopes. Models 1 and 2 are given in the first row, while Models 3 and 4 are given in the second row, and Models 5 and 6 are given in the third row and finally Models 7 and 8 are given in the fourth row from left to right, respectively. The color codes are the same as Figure 1 and Table 1.

HO potential are selected only for the isotopes which are weakly influenced by the shell effects. This situation is also consistent with the issue which is mentioned above in the discussion of Figure 1 as well as Table 2. However, Model 6 has been selected around the closed shell near the mass number A equal to 208, this contradiction is caused by the fact that the demand to select the model which gives the deepest peak in this region. Similarly, around the open shells, the selections have been a model including Coulomb term but this time it is Model 4 or 8, which gives the highest peak in these regions. Therefore, it can be concluded from Figure 4 that it is essential to consider Coulomb interaction for the isotopes around both closed and open shells.

Finally, Figure 5 represents the asymptotic level density parameter values for nuclei, which are known as superheavy elements, in the mass region $Z > 100$. The upper panel includes the comparison between Models 5 and 6 to discuss the effect of Coulomb term in this mass region. It

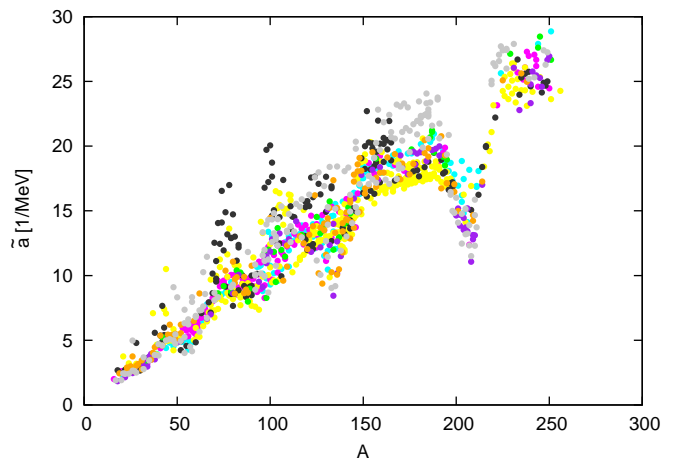


Fig. 4. (Color online) The asymptotic level density parameter values obtained by using Model 0, which is the local selections of the global parameterizations of Models 1-8. The color codes are the same as Figure 1 and Table 1.

can be clearly seen that Coulomb term has an inhibitory effect on the asymptotic level density parameter for the increasing proton numbers. To discuss the effect of the deformation, the comparison between Models 3 and 7 is given in the lower panel. The values resulting from Model 7, which is the deformed version of Model 3, are slightly greater than the predictions of Model 3. On the other hand, one can easily say that the asymptotic level density parameter tends to reach a limit value with the increasing mass number.

To extract the asymptotic value of the level density parameter for a certain superheavy nucleus, one can easily use the conservation condition (12) with the selected single particle potential and compute the Fermi energy. Thus, asymptotic level density parameter can be calculated by using Eq. (10), which also includes the shell and pairing corrections. While the pairing correction energy can be calculated from its traditional definition (see the text after Eq. (10)), the calculated shell correction energies with the liquid drop model [18] by using the parameter values as in Ref. [19] are given in Figure 6. As expected, a strong correlation between \tilde{a} and $S(N, Z)$ values is observed from Figs. 5 and 6. Therefore, a reliable extrapolation to the nuclei far from stability requires both a well-defined single-particle potential and a parameter set for liquid drop model. Because of the fact that the energy dependence of the level density parameter is completely defined by the collective amplitude A_c , deformation parameters are required for both obtaining $a(U)$ and an asymptotic value of the level density parameter with deformed single-particle models. The calculated values of the deformation parameters with Finite Range Droplet Model [34] are used for nuclei where experimental information is not available.

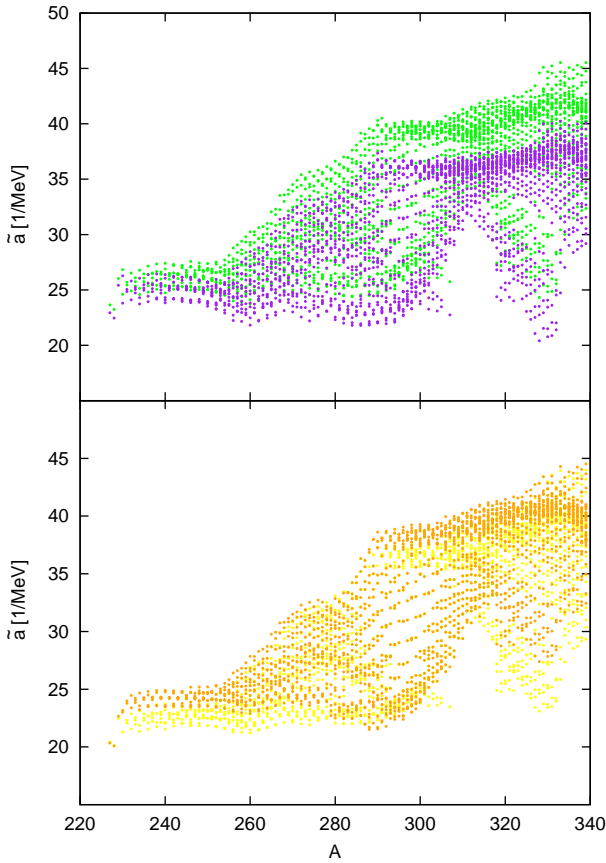


Fig. 5. (Color online) The asymptotic level density parameter values for superheavy nuclei, which have atomic number $Z > 100$. The upper and lower panels represent the comparisons between Models 5 and 6, and Models 3 and 7, respectively. The color codes are the same as Figure 1 and Table 1.

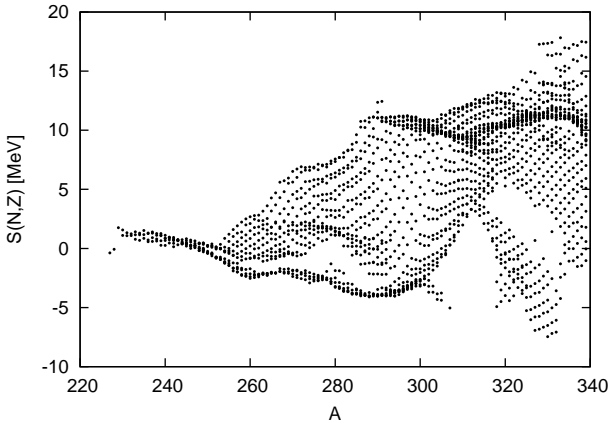


Fig. 6. The shell correction energies for superheavy nuclei. The liquid drop model parameters are taken as in Ref. [19].

6 Conclusions

Summarizing, the effect of the single-particle potential terms, which are central, spin-orbit, harmonic oscillator, Woods-Saxon and Coulomb potential, both for spherical and deformed cases, on the level density parameter was

investigated by examining the local success of the global parameterizations of eight different combinations of these terms. In the light of above discussions, the following conclusions can be drawn from this study:

- (i) Model 2, which is the sum of the central, spin-orbit, harmonic oscillator and Coulomb potentials, gives the most accurate predictions compared to experimental data.
- (ii) The local selections of the global parameterizations indicate that the single-particle models, which are based on Woods-Saxon potential as the main term, are more suitable candidates than the models based on harmonic oscillator potential to extrapolate away far from stability.
- (iii) It is seen from the investigation of the asymptotic level density parameters obtained from the local selection that the contribution of Coulomb interaction is not ignorable both around the closed and open shells.
- (iv) Finally, for the exotic and superheavy nuclei, which have not any experimental information to adjust the level density parameters, the single-particle potential consists of the central, spin-orbit, Woods-Saxon, and Coulomb potential terms is the most reliable potential model to calculate the asymptotic level density parameter.

Acknowledgements

This work was supported by the Turkish Science and Research Council (TÜBİTAK) under Grant No. 112T566. Bora Canbula acknowledges the support through TÜBİTAK PhD Program fellowship BİDEB-2211 Grant.

References

1. I. Tanihata, H. Hamakagi, O. Hashimoto, Y. Shida, N. Yoshikawa, K. Sugimoto, O. Yamakawa, T. Kobayashi, N. Takahashi, *Phys. Rev. Lett.* **55**, 2676-2679 (1985).
2. G.R. Satchler, *Direct Nuclear Reactions*, Clarendon Press, Oxford (1983).
3. T. Tamura, *Rev. Modern Phys.* **37**, 679-708 (1965).
4. W. Tobocman, M.H. Kalos, *Phys. Rev.* **97**, 132-136 (1955).
5. G.H. Rawitscher, *Phys. Rev. C* **9**, 2210-2229 (1974).
6. Y. Sakuragi, M. Yahiro, M. Kamimura, *Prog. Theoret. Phys.* **68**, 322-326 (1982).
7. Y. Sakuragi, Y. Masanobu, K. Masayasu, *Prog. Theo. Phys. Suppl.* **89**, 136-211 (1986).
8. Y. Yamagata, K. Yuasa, N. Inabe, M. Nakamura, M. Tanaka, S. Nakayama, K. Katori, M. Inoue, S. Kubono, T. Itahashi, H. Ogata, Y. Sakuragi, *Phys. Rev. C* **39**, 873-876 (1989).
9. B. Sinha, *Phys. Rep.* **1**, 1-57 (1975).
10. G.R. Satchler, W.G. Love, *Phys. Rep.* **3**, 183-254 (1979).
11. V. Lapoux et al., *Phys. Lett. B* **658**, 198-202 (2008).
12. B. Canbula, R. Bulur, D. Canbula, H. Babacan, *Nuclear Physics A* **929**, 54-70 (2014).
13. B. Canbula, H. Babacan, *Nucl. Phys. A* **858**, 32-47 (2011).

14. R. Capote et al., Nucl. Data Sheets **110**, 3107-3214 (2009).
15. H.A. Bethe, Rev. Mod. Phys. **9**, 69 (1937).
16. H. Hagehund, A.S. Jensen, Phys. Scr. **15**, 225-236 (1977).
17. A.V. Ignatyuk, *The Statical Properties of the Excited Atomic Nuclei*, Energoatomizdat, Moscow (1983).
18. W.D. Myers, W.J. Swiatecki, Nucl. Phys. **81**, 1-60 (1966).
19. A. Mengoni, Y. Nakajima, J. Nucl. Sci. Tech. **31**, 151-162 (1994).
20. D.J. Rowe, *Nuclear Collective Motion*, Methuen, London (1970).
21. K.S. Krane, *Introductory Nuclear Physics*, John Wiley and Sons Inc. (1987).
22. P. Ring, P. Schuck, *The Nuclear Many-Body Problem*, Springer (1980).
23. K. Siegbahn, *Alpha-, Beta- and Gamma-Ray Spectroscopy*, North-Holland (1965).
24. T. Ericson, Adv. Phys. **9**, 425-511 (1960).
25. J. Bartel, K. Pomorski, B. Nerlo-Pomorska, Int. J. Mod. Phys. E **15**, 478-483 (2006).
26. A.S. Iljinov, M.V. Mebel, N. Bianchi, E. De Sanctis, C. Guaraldo, V. Lucherini, V. Muccifora, E. Polli, A.R. Reolon, P. Rossi, Nucl. Phys. A **543**, 517-557 (1992).
27. A. Bohr, B.R. Mottelson, *Nuclear Structure*, W. A. Benjamin, Inc. (1998).
28. M. Brack, R.K. Bhaduri, *Semiclassical Physics*, Addison-Wesley Publishing Company, Inc. (1997).
29. L. Salasnich, J. Math. Phys. **41**, 8016-8024 (2000).
30. W. Greiner, J.A. Maruhn, *Nuclear Models*, Springer-Verlag (1996).
31. T. Bayram, S. Akkoyun, S.O.Kara, A. Sinan, Acta Phys. Pol. B **44**, 1971-1799, (2013).
32. I. Angeli, K.P. Marinova, At. Nucl. Data Tables **99**, 69-95 (2013).
33. A.V. Ignatyuk, G.N. Smirenkin, A.S. Tishin, Sov. J. Nucl. Phys. **21**, 255 (1975).
34. P. Moller, J.R. Nix, W.D. Myers, W.J. Swiatecki, At. Nucl. Data Tables **59**, 185 (1995); P. Moller, J.R. Nix, At. Nucl. Data Tables **26**, 165 (1981); G. Audi, A.H. Wapstra, C. Thibault, Nucl. Phys. A **729**, 337 (2003).